International Journal of Engineering

Synthesis and Characterization of Highly Porous TiO₂ Scaffolds for Bone Defects

S. M. Mirhadi, N. Hassanzadeh Nemati*

Department of Biomedical engineering, Science and Research Branch, Islamic Azad University, Tehran, Iran

A B S T R A C T

The purpose of this study was to fabricate and investigate the highly porous structure using titanium dioxide, which is a candidate for bone defect repairing. For this purpose, TiO₂ scaffolds were synthesized using titanium butoxide, Pluronic F127 surfactant, and polyurethane foam blocks. Therefore, a colloid includes titanium butoxide and F127 and the polyurethane foams were immersed in it. The samples were annealed at different temperatures in the range of 500 to 600 °C. The results of simultaneous thermal analysis (STA) test showed that volatile materials left the system completely when the temperature reached 550 ℃. Also, small angle X-ray scattering (SAXS) test revealed that these scaffolds composed of highly ordered mesoporous structures. The obtained scaffolds at 550 ℃ had specific surface area of 85.736 m2g-1with the mean mesopore size of 7.0498 nm and macroporosity in the range of 100 to 350 μm. The presence of mesopores and their distribution were investigated with transmission electron microscopy (TEM) and energy dispersive spectroscopy (EDS). The base scaffold was then immersed in a simulated body solution for 3,7and 14 days and analyzed by scanning electron microscopy (SEM) and energy-dispersive X-ray. The results show its ability for apatite formation.

doi: 10.5829/ije.2020.33.01a.15

1. INTRODUCTION

Bone is a 3D and porous structure. These porosities provide the required spaces to establish, connect, nourish and perform other metabolic activities of cells. Furthermore, the porous structure prepares a desired environment for regeneration and remodeling of broken bones or defects in their structures [1-3]. Bone tissue engineering offers new solutions to treat many problems such as fracture, osteoporosis or bone defects. Hence, engineered bone scaffolds will be successful if they can mimic the extracellular matrix (ECM) and the 3D structure of real bone [4, 5]. An appropriate interface with proper characteristics can provide a suitable environment for positive interaction between the scaffolds constituents

and living tissue cells. The presence of macroporosity in the range of 100 to 1000 micron causes the biological relevance such as cell proliferation, growth, and migration into the porosities [6]. Modification of pore wall surfaces affects topography, surface energy, reactivity and biofunctionality of the scaffolds [7, 8]. Loading and delivery of nanomaterials such as proteins, growth factors, ligands and DNA with the size of 10-100 nm for biomedical applications depend on nano-roughness, mesoporosity, and high specific surface area in adjacent to cell environment [4, 9-13].

Titanium dioxide has various biomedical applications [14-18]. TiO₂ with high specific surface area can mimic the properties of extra cellular matrix (ECM) by bonding to proteins and apatite and provides a platform to attach

*Corresponding Author Email: hasanzadeh@srbiau.ac.ir (N. Hassanzadeh Nemati)

to osteoblasts [14-19]. Titania with mesoporous structure can be synthesized using titanium alkoxides such as titanium butoxide and other additives similar to Pluronic F127 surfactant utilizing evaporation-induced self-assembly technique (EISA) [20-23]. On the other hand, macropores in the range of 1-1000 micron can be produced with various techniques including sponge matrix imbedding [6, 24, 25].

In this study, we synthesized and characterized highly porous TiO₂ scaffolds with a meso/macroporous structure by combining two aforementioned techniques, evaporation-induced self-assembly (EISA) and PU replica foams method. For this purpose, TiO₂ colloidal sol was prepared using titanium butoxide precursor and F127 surfactant. Finally, meso/macropores was induced in PU foam after heat treatment of the specimens. The samples were characterized and the formation mechanism involved in this process was scrutinized as well. The benefits of this method of fabrication include porosity for loading cells, biological agents and drugs, as well as ease of manufacture and high purity.

2. MATERIALS AND METHODS

2. 1. Sample Preparation   Titanium butoxide (abbreviated as TBT, C16H36O4Ti, 97%, Sigma Aldrich) and F127 copolymer (99.5%, Sigma Aldrich) were used as a precursor and template, respectively. Anhydrous ethanol (abbreviated as EtOH, C2H6O, 99.5%, Sigma Aldrich), hydrochloric acid (HCl, 38 wt.%) and acetylacetone (abbreviated as AcAc, C5H8O2, 99.5%, Sigma Aldrich) were utilized as solvent and to restrain the hydrolysis rate. The initial materials were mixed according to the study performed by Li et al. [25]. Briefly, a colloidal solution of F127/TBT/HCl/EtOH/AcAc with the weight ratio of 2/5/8/100/3 was prepared and aged for 2 days at room temperature with relative humidity of 40%. Pre-cut foam blocks of PU with 60 pore per inch (ppi) with the dimension of 1cm× 1cm× 1cm were soaked in colloidal solution for 2 min. The ratio between the initial materials was reported to be an efficient one to produce TiO₂ mesoporous structure with high thermal stability during required heat treatment to remove PU foams [25]. In the next step, to replicate the foam structure and to remove the extra colloidal solution, the samples were rolled and dried in closed containers at room temperature for 72 h. Finally, the samples were heat treated at 500, 550, 600 ℃ for 2 h with the heating/cooling rate of 4 ℃/min. The synthesis procedure is schematically shown in Figure 1.

2. 2. Characterization of TiO₂ Scaffolds   Small-angle X-ray scattering (SAXS) and wide-angle X-ray diffraction (WAXD) patterns were recorded using Asenware AW-DX300 with a Cu Kα radiation source

with λ = 1.54184 Aº with 2θ in the range of 0.5-10 degree for SAXS and 10-100 degree for WAXD using Asenware AWDX300 diffractometer. In order to study the weight loss and to monitor any exo/endothermic reaction during the heat treatment cycle, simultaneous thermal analysis (STA) was performed up to 550 ℃ with the heating rate of 10 ℃/min in air atmosphere using NETZSCH STA 449F3 machine. To analyze pore structure and to evaluate the specific surface area, the nitrogen adsorption–desorption isotherms was obtained at 77 K using BELSORP-mini II analyzer. Pore size, morphology, interconnectivities and their distribution were studied using scanning electron microscope (SEM/EDS, Zeiss, Germany and FEI Quanta 200. Nanostructures and mesopores on the wall of macropores of TiO₂ scaffolds, were analyzed using transition electron microscope (TEM JEM- 100CXI). Finally, the porous scaffolds were immersed in the simulated body (purchased from Apra-Chem Co.) for 3,7,14 days in the solution by combining Table 1. Apatite formation ability on the scaffold was then investigated using scanning microscope, FEI Quanta 200 and EDX.
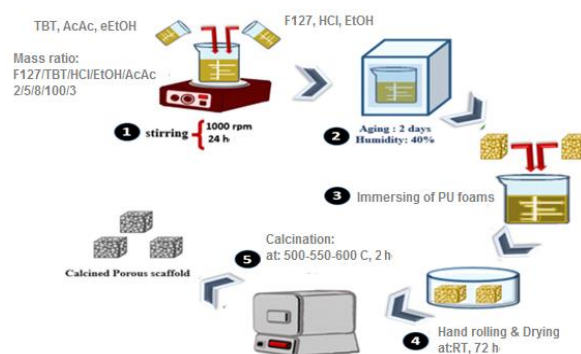

Figure 1. The synthesis procedure of TiO₂ scaffolds during 6 steps as mentioned in section 2.1

TABLE 1. Composition and concentration of SBF

ION	Concentration mM/10⁻⁴m³
Na⁺	14.2
K⁺	0.5
Mg₂⁺	0.15
Ca₂⁺	025
Cl⁻	14.78
HCO₃⁻²	0.42
HPO₄⁻²	0.1
SO3⁻²	0.05

3. RESULTS AND DISCUSSION

3. 1. X-Ray Analyses   Figure 2a shows the small-angle X-ray scattering (SAXS) of various samples after sintering at high temperature. As seen, an intense peak exists in 0.7 degree in the sample sintered at 500 ºC. The specimen sintered at 550 ºC also showed the same peak with lower intensity. The presence of the peak demonstrates the existence of mesoporous structure in these samples; however the decrease of the peak intensity can be referred to the decrease of the size of mesopores [21]. In the sample sintered at 600 ºC, the intensity of the peak reduced drastically which shows the collapse of mesoporous structure. In order to make sure all the volatile materials were removed from the scaffold structure (and based on the results of STA), samples sintered at 550 ºC were selected for further studies. Wide-angle X-ray diffraction (WAXD) of various specimens has been shown in Figure 2b. All the peaks correspond to the characteristic peaks of TiO_2 (XRD JCPDS data file No. 02-0387). When increasing the temperature, from 500 to 600 ºC, the intensity of XRD peaks increased as a result of crystallization of the samples [26]. Hiraj et al. [27] reported the TiO_2 formation mechanism which consists of three stages. At the first stage, the alkoxide is hydrolyzed according to the following reaction [27]:

$$C_{16}H_{36}O_4Ti + 4H_2O \rightarrow Ti(OH)_4 + 4C_4H_9OH \qquad (1)$$

Then, the hydrolyzed species are condensed to form TiO_2 particles:

$$Ti(OH)_4 \rightarrow TiO_2 + 2H_2O \qquad (2)$$

The next step is the formation of nuclei from the hydrolyzed molecules. Formation of small nuclei is accompanied with the formation of huge surface area and consequently huge surface energy which makes them thermodynamically unstable. As a result, a few numbers of nuclei attach to each other to decrease the system energy and form a stable state. Finally, agglomeration and Ostwald ripening cause the formation of larger particles. Furthermore, the newly hydrolyzed molecules precipitate on the surface of previously formed particles. Agglomeration occurs due to the existing Brownian motion and coagulation of the particles. Finally, in Ostwald ripening the larger particles grow at the expense of smaller particles until the smaller particles completely vanished in the system [27, 28].

3. 2. Thermal Analysis   Simultaneous thermal analysis (STA) was performed to evaluate the thermal behavior of scaffolds during the synthesis process. Figure 3a shows the results of STA analysis of prepared colloidal solution before soaking in PU foam. As seen, an endothermic peak exists at 80.4 ºC which can be ascribed to the remove of solvent from the system. Two exothermic peaks were observed at 200.2 and 314.8 ºC which can be attributed to the oxidation of organic

materials such as surfactant and calcination of butyl titanate, respectively. A total weight loss of 74.28% was detected in this sample. Figure 3b shows the TG/DSC curve of the produced sample in the presence of PU foams. The effect of adding PU foams to the system can be understood by comparing Figures 3a and b. The same endothermic peak was obtained at 80.6 ºC as a result of the remove of solvent from the system. PU foams increased the exothermic peaks to 267.2 and 314.8 ºC, respectively. In the DSC curve, in addition to the mentioned peaks, another peak was distinguished at 422 ºC due to the remove of PU foam. As can be seen in the TG curve, no weight loss was observed after 500 ºC which shows all the volatile materials were removed from the system. The total weight loss obtained in this sample was 81.96%.

3. 3. Nitrogen Adsorption–Desorption Analysis
The nitrogen adsorption–desorption isotherm of produced samples after annealing at 550 ºC for 2 h is shown in Figure 4. As seen, the physiosorption isotherm showed a hysteresis loop which is associated with capillary condensation and is of the type IV isotherm according to the IUPAC classification [29]. The hysteresis loop is similar to H4 which is due to the presence of slit-shape mesopores [29-31]. The specific
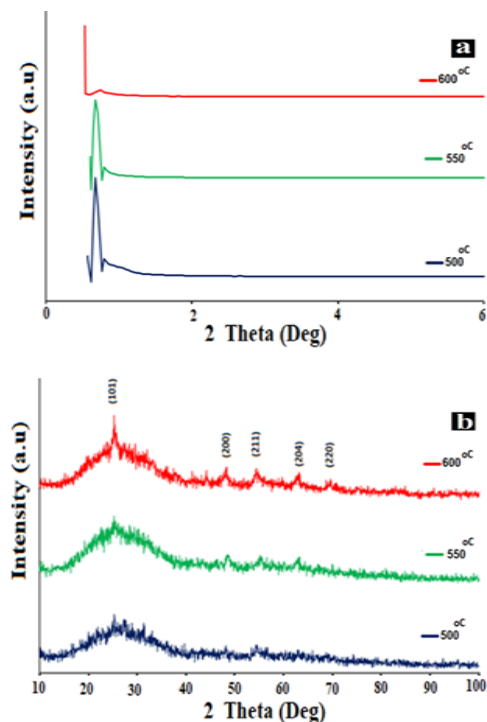
Figure 2. X-ray diffraction patterns at (a) Small angles and (b) wide-angles for the TiO_2 samples sintered at various temperatures for 2 h holding time
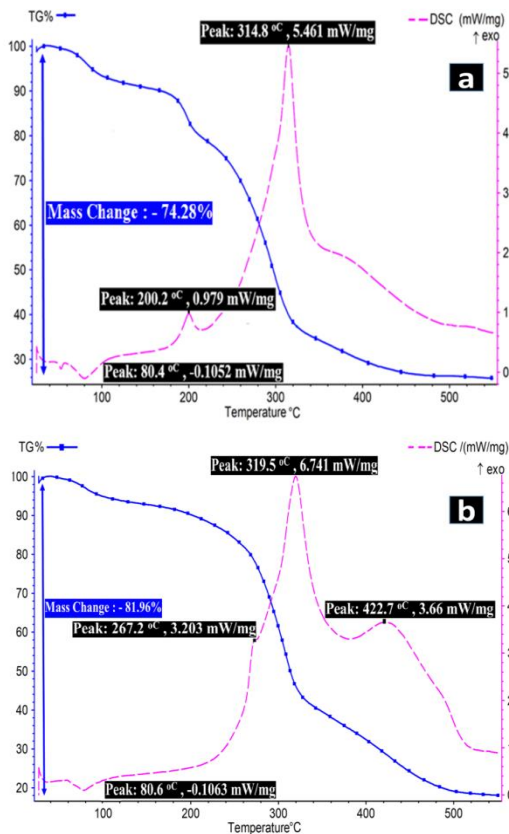
Figure 3. Simultaneous thermal analysis of colloidal solution including surfactant (a) in the absence and b) in the presence of PU foam

surface area measured by Brunauer-Emmett-Teller (BET) theory for this sample was 85.736 m^2g-1, the total porosity volume obtained from adsorption curve of isotherm diagram (p/p_0=0.990) and mean pore diameter were 0.1511 cm3g-1 and 7.0498 nm, respectively.

3. 4. SEM Analysis   The morphology, size, interconnectivity and thickness of the pore walls of samples sintered at 550 ºC for 2h are shown in Figure 5. The size of macropores was in the range of 100-350 μm which allows efficient cell accommodation inside the porosity [32]. The thickness of the pore walls was in the range of 10-30 μm. As seen, a coherent structure was formed without any cracks after sintering the specimens at 550 ºC for 2h. Such a structure can provide a desirable environment for cell growth and proliferation [12]. Figure 6 shows the structure of pore walls in different magnifications. The size of pores was distributed from several nanometer to over 100 nm. As seen, mesopores can be observed within the structure which confirmed the results obtained from SAXS and nitrogen adsorption–desorption analysis.

3. 5. Tem Analysis   The morphology of TiO_2 sample after sintering at 550 ºC for 2 h is shown in Figure 7. Figures 7a to 7d shows the existence of mesopores on the samples. The size of mesopores and their wall thickness were in the range of 10-12 nm and 5-15 nm,
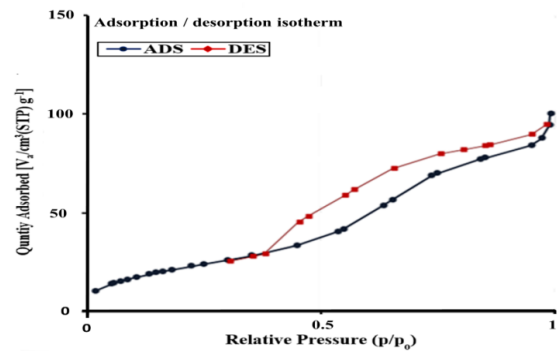

Figure 4. Nitrogen adsorption–desorption isotherms of TiO_2 samples after sintering at 550 ºC for 2 h
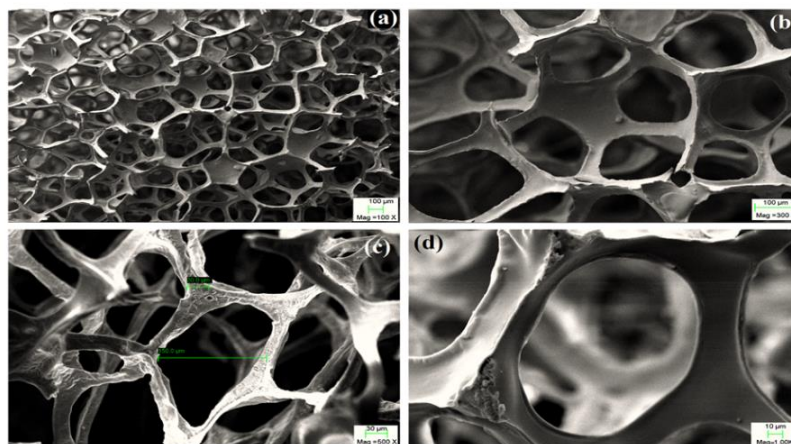

Figure 5. SEM micrographs of TiO_2 scaffolds at different magnifications (a) 100×, (b) 300×, (c) 500×, and (d) 1000×
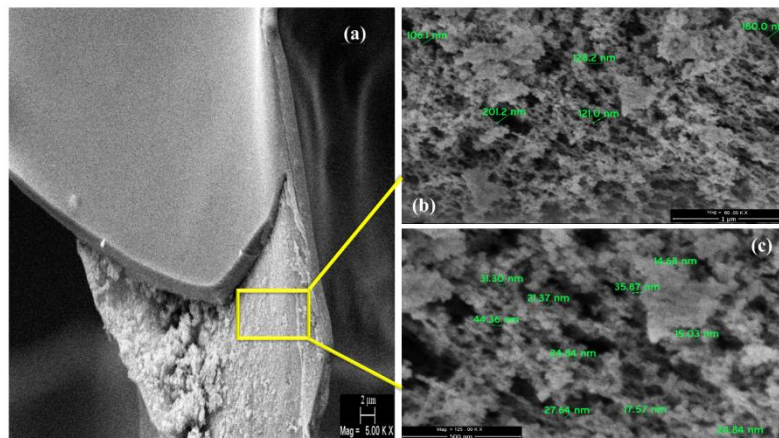
Figure 6. SEM micrographs of macropore wall in the produced TiO₂ scaffolds at different magnifications (a) 5k×, (b) 60k×, and (c) 125k×
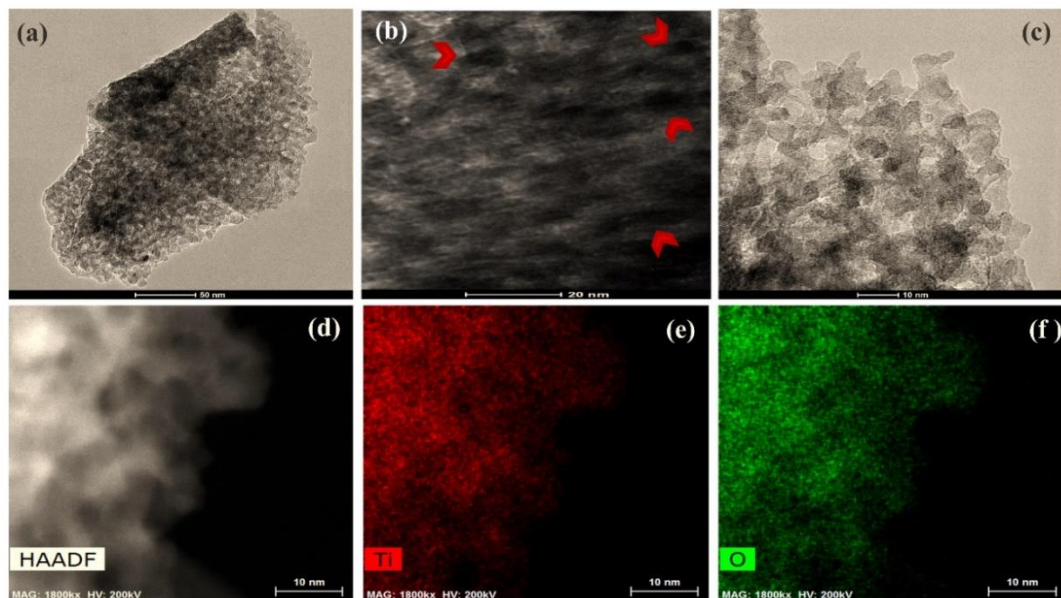

Figure 7. (a-c) TEM micrographs of mesopores in the produced TiO2 scaffolds after sintering at 550°C for 2 h at different magnifications; with two different magnifications. d) High-angle annular dark-field scanning transmission electron microscopy (HAADF-STEM) image of the specimen. EDS elemental maps of the failure surface of the sample (e) titanium and (f) oxygen

respectively. The EDS analysis (Figures 7e and 7f) showed the uniform distribution of titanium and oxygen on the samples.

3. 6. In-vitro Bioactivity of Porous Titania Scaffolds   Apatite formation in simulated body solution on the porous scaffold is one of the ways of bioactivity study. Therefore, the scaffolds were immersed in simulated body solution for 3, 7days using scanning electron microscopy Investigation (Figure 8).

Figure 8 shows EDX analysis and susceptibility of the produced scaffolds to apatite growth on the surface of the macroporous arms (containing mesoporous) with 3, 7, and 14 days of immersion in the simulated body solution.

4. CONCLUSION

TiO₂ scaffolds with high specific surface area were produced by combining evaporation-induced self-assembly (EISA) technique and PU replica foams method. In this study, Pluronic F127 surfactant and polyurethane foams were used to induce meso and macro porosities, respectively.

These organic materials left the system after sintering the samples at 550 °C for 2 h. The produced scaffold had macropores in the range of 100-300 μm and mesopores of about 10-12 nm. The surface of the obtained scaffolds had nano-topography in the range of 100-250 nm which provided a high specific surface area of 85.736 m²g⁻¹.
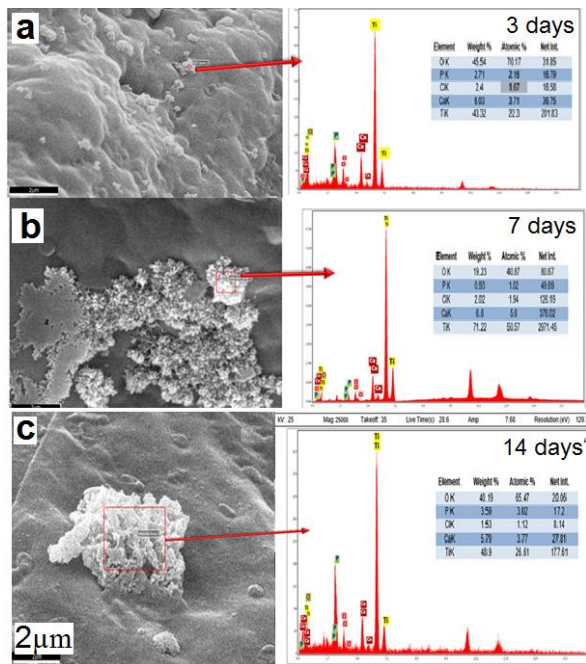
Figure 8. SEM micrographs and EDX analysis of apatite growth on the surface of the macroporous arms (containing mesoporous) after (a) 3, (b) 7, and (c) 14 days immersion in the simulated body solution

The results represent of meso-and macroporous forming techniques in titanium scaffolding provides a high surface area and porosity for the loading of biological agents and cells required for bone growth.

5. REFERENCES

1. Reznikov, N., Shahar, R. and Weiner, S., "Bone hierarchical structure in three dimensions", *Acta Biomaterialia*, Vol. 10, No. 9, (2014), 3815-3826.

2. Gibon, E., Lu, L.Y., Nathan, K. and Goodman, S.B., "Inflammation, ageing, and bone regeneration", *Journal of Orthopaedic Translation*, Vol. 10, (2017), 28-35.

3. Ralston, S.H., "Bone structure and metabolism", *Medicine*, Vol. 45, No. 9, (2017), 560-564.

4. Ma, P.X., "Biomimetic materials for tissue engineering", *Advanced Drug Delivery Reviews*, Vol. 60, No. 2, (2008), 184-198.

5. El-Rashidy, A.A., Roether, J.A., Harhaus, L., Kneser, U. and Boccaccini, A.R., "Regenerating bone with bioactive glass scaffolds: A review of in vivo studies in bone defect models", *Acta Biomaterialia*, Vol. 62, (2017), 1-28.

6. Dutta, R.C., Dey, M., Dutta, A.K. and Basu, B., "Competent processing techniques for scaffolds in tissue engineering", *Biotechnology Advances*, Vol. 35, No. 2, (2017), 240-250.

7. Roseti, L., Parisi, V., Petretta, M., Cavallo, C., Desando, G., Bartolotti, I. and Grigolo, B., "Scaffolds for bone tissue engineering: State of the art and new perspectives", *Materials Science and Engineering: C*, Vol. 78, (2017), 1246-1262.

8. Bose, S., Robertson, S.F. and Bandyopadhyay, A., "Surface modification of biomaterials and biomedical devices using additive manufacturing", *Acta Biomaterialia*, Vol. 66, (2018), 6-22.

9. Tang, W., Lin, D., Yu, Y., Niu, H., Guo, H., Yuan, Y. and Liu, C., "Bioinspired trimodal macro/micro/nano-porous scaffolds loading rhbmp-2 for complete regeneration of critical size bone defect", *Acta Biomaterialia*, Vol. 32, (2016), 309-323.

10. Wu, C., Zhou, Y., Chang, J. and Xiao, Y., "Delivery of dimethyloxallyl glycine in mesoporous bioactive glass scaffolds to improve angiogenesis and osteogenesis of human bone marrow stromal cells", *Acta Biomaterialia*, Vol. 9, No. 11, (2013), 9159-9168.

11. Lozano, D., Manzano, M., Doadrio, J.C., Salinas, A.J., Vallet-Regí, M., Gómez-Barrena, E. and Esbrit, P., "Osteostatin-loaded bioceramics stimulate osteoblastic growth and differentiation", *Acta Biomaterialia*, Vol. 6, No. 3, (2010), 797-803.

12. Yi, H., Rehman, F.U., Zhao, C., Liu, B. and He, N., "Recent advances in nano scaffolds for bone repair", *Bone Research*, Vol. 4, (2016), 16050.

13. Chen, H., Huang, X., Zhang, M., Damanik, F., Baker, M.B., Leferink, A., Yuan, H., Truckenmüller, R., van Blitterswijk, C. and Moroni, L., "Tailoring surface nanoroughness of electrospun scaffolds for skeletal tissue engineering", *Acta Biomaterialia*, Vol. 59, (2017), 82-93.

14. Gongadze, E., Kabaso, D., Bauer, S., Slivnik, T., Schmuki, P., Van Rienen, U. and Iglič, A., "Adhesion of osteoblasts to a nanorough titanium implant surface", *International Journal of Nanomedicine*, Vol. 6, (2011), 1801.

15. Zhang, P., Zhang, Z., Li, W. and Zhu, M., "Effect of ti-oh groups on microstructure and bioactivity of tio2 coating prepared by micro-arc oxidation", *Applied Surface Science*, Vol. 268, (2013), 381-386.

16. Han, G., Müller, W.E., Wang, X., Lilja, L. and Shen, Z., "Porous titania surfaces on titanium with hierarchical macro-and mesoporosities for enhancing cell adhesion, proliferation and mineralization", *Materials Science and Engineering: C*, Vol. 47, (2015), 376-383.

17. Chen, Y., Zheng, X., Ji, H. and Ding, C., "Effect of ti–oh formation on bioactivity of vacuum plasma sprayed titanium coating after chemical treatment", *Surface and Coatings Technology*, Vol. 202, No. 3, (2007), 494-498.

18. Tiainen, H., Wohlfahrt, J.C., Verket, A., Lyngstadaas, S.P. and Haugen, H.J., "Bone formation in tio2 bone scaffolds in extraction sockets of minipigs", *Acta Biomaterialia*, Vol. 8, No. 6, (2012), 2384-2391.

19. Haugen, H.J., Monjo, M., Rubert, M., Verket, A., Lyngstadaas, S.P., Ellingsen, J.E., Rønold, H.J. and Wohlfahrt, J.C., "Porous ceramic titanium dioxide scaffolds promote bone formation in rabbit peri-implant cortical defect model", *Acta Biomaterialia*, Vol. 9, No. 2, (2013), 5390-5399.

20. Pan, J.H., Zhao, X. and Lee, W.I., "Block copolymer-templated synthesis of highly organized mesoporous tio2-based films and their photoelectrochemical applications", *Chemical Engineering Journal*, Vol. 170, No. 2-3, (2011), 363-380.

21. Li, H., Wang, J., Li, H., Yin, S. and Sato, T., "High thermal stability thick wall mesoporous titania thin films", *Materials Letters*, Vol. 63, No. 18-19, (2009), 1583-1585.

22. Bagheri, S., Hir, Z.A.M., Yousefi, A.T. and Hamid, S.B.A., "Progress on mesoporous titanium dioxide: Synthesis, modification and applications", *Microporous and Mesoporous Materials*, Vol. 218, (2015), 206-222.

23. Mahoney, L. and Koodali, R., "Versatility of evaporation-induced self-assembly (eisa) method for preparation of mesoporous tio2 for energy and environmental applications", *Materials*, Vol. 7, No. 4, (2014), 2697-2746.

24. Haugen, H., Will, J., Köhler, A., Hopfner, U., Aigner, J. and Wintermantel, E., "Ceramic tio2-foams: Characterisation of a potential scaffold", *Journal of the European Ceramic Society*, Vol. 24, No. 4, (2004), 661-668.

25. Studart, A.R., Gonzenbach, U.T., Tervoort, E. and Gauckler, L.J., "Processing routes to macroporous ceramics: A review", *Journal of the American Ceramic Society*, Vol. 89, No. 6, (2006), 1771-1789.

26. Tavangarian, F. and Emadi, R., "Mechanical activation assisted synthesis of pure nanocrystalline forsterite powder", *Journal of Alloys and Compounds*, Vol. 485, No. 1-2, (2009), 648-652.

27. Hirai, T., Sato, H. and Komasawa, I., "Mechanism of formation of titanium dioxide ultrafine particles in reverse micelles by hydrolysis of titanium tetrabutoxide", *Industrial & Engineering Chemistry Research*, Vol. 32, No. 12, (1993), 3014-3019.

28. Guozhong, C., "Nanostructures and nanomaterials: Synthesis, properties and applications, World scientific, (2004).

29. Sing, K.S., "Reporting physisorption data for gas/solid systems with special reference to the determination of surface area and porosity (recommendations 1984)", *Pure and Applied Chemistry*, Vol. 57, No. 4, (1985), 603-619.

30. ALOthman, Z., "A review: Fundamental aspects of silicate mesoporous materials", *Materials*, Vol. 5, No. 12, (2012), 2874-2902.

31. Li, X.-Y., Chen, L.-H., Rooke, J.C., Deng, Z., Hu, Z.-Y., Wang, S.-Z., Wang, L., Li, Y., Krief, A. and Su, B.-L., "Mesoporous titanium dioxide (tio2) with hierarchically 3d dendrimeric architectures: Formation mechanism and highly enhanced photocatalytic activity", *Journal of Colloid and Interface Science*, Vol. 394, (2013), 252-262.

32. Karageorgiou, V. and Kaplan, D., "Porosity of 3d biomaterial scaffolds and osteogenesis", *Biomaterials*, Vol. 26, No. 27, (2005), 5474-5491.

Synthesis and Characterization of Highly Porous TiO₂ Scaffolds for Bone Defects

S. M. Mirhadi, N. Hassanzadeh Nemati*

Department of Biomedical engineering, Science and Research Branch, Islamic Azad University, Tehran, Iran

چکیده

هدف از این مطالعه ساخت و بررسی ساختار بسیار متخلخل دی اکسید تیتانیوم است که کاندیدایی برای ترمیم نقص استخوان است. برای این منظور، داربست‌های TiO₂ با استفاده از تیتانیوم بوتوکسید، سورفکتانت Pluronic F127 و بلوک‌های اسفنجی پلی‌اورتان سنتز شدند. برای این منظور فوم پلی‌اورتان در محلول کلوئیدی تیتانیوم بوتوکسید غوطه‌ور شدند. نمونه‌ها در دماهای مختلف در دامنه‌ی ۵۰۰ تا ۶۰۰ درجه‌ی سانتی‌گراد آنیل شدند. نتایج حاصل از آزمایش آنالیز حرارتی همزمان (STA) نشان داد که مواد فرار با رسیدن به دمای ۵۵۰ درجه‌ی سانتی‌گراد سیستم را کاملاً ترک می‌کند. همچنین، آزمون پراکندگی با پرتوی ایکس زاویه‌ی کوچک (SAXS) نشان داد که این داربست‌ها از ساختارهای مزوپور بسیار مرتب تشکیل شده‌اند. داربست‌های بدست‌آمده در دمای ۵۵۰ درجه‌ی سانتی‌گراد از سطح ویژه‌ی m2g-1 ۸۵٬۷۳۶ با حفره‌های مزو با میانگین اندازه‌ی ۷.۰۴۹۸ نانومتر و تخلخل‌های ماکرو در محدوده‌ی ۱۰۰ تا ۳۵۰ میکرومتر برخوردار بودند. حضور مزوپورها و توزیع آنها با میکروسکوپ الکترونی عبوری (TEM) و طیف‌سنجی پراکندگی انرژی (EDS) بررسی شد. سپس، داربست پایه در یک محلول شبیه‌سازی‌شده بدن به مدت ۳.۷ و ۱۴ روز غوطه‌ور شد و توسط میکروسکوپ الکترونی روبشی (SEM) و پرتوی ایکس پراکنده انرژی تحلیل شد. نتایج نشان‌دهنده‌ی توانایی آن در تشکیل آپاتیت است.

doi: 10.5829/ije.2020.33.01a.15